JACS Au
AN OPEN ACCESS JOURNAL OF THE AMERICAN CHEMICAL SOCIETY

pubs.acs.org/jacsau
Article

Deep Profiling of Oocyte Aging Enabled by Simple One-Step Vial-Based Pretreatment and Single-Cell Proteomics

Hui Zhang,[#] Hailu Zhang,[#] Chuanxi Huang,[#] Qing Zeng, Chunyan Tian, Jing Yang, Fuchu He,[*] and Yun Yang[*]

Cite This: *JACS Au* 2025, 5, 2321−2333
Read Online

ABSTRACT: Single-cell proteomics is a pivotal technology for studying cellular phenotypes, offering unparalleled insights into cellular heterogeneity and dynamic functions. Technical improvement in mass spectrometry instruments and sample preparation has made proteomics profiling of single mouse oocytes or early embryos feasible in recent years. Yet, developing a simple and robust sample preparation method to enable deep proteomics profiling of single germline cells remains a significant challenge. Herein, we developed a simple one-step vial-based pretreatment (SOViP) for deep label-free single-cell proteomics of germline cells. SOViP integrates all sample preparation procedures into a single step in autosampler vials, yet it is highly efficient and high-throughput in comparison to reported multistep methods. SOViP can be finished within ∼2 h with hands-on time limited to merely a few minutes. On average, over 6500 protein groups can be quantified from a single mouse oocyte using SOViP. In total, 6983 protein groups were identified from single mouse oocytes across an entire reproductive lifespan, offering a valuable proteomics resource for oocyte aging. Unique molecular characteristics of oocytes at different ages were revealed, and a classifier consisting of ten proteins demonstrated accurate age-group classification and fertility-level prediction. Although demonstrated using mouse oocytes in this study, SOViP is adaptable to rare cell samples and other large cells including follicles and preimplantation embryo cells, among others.

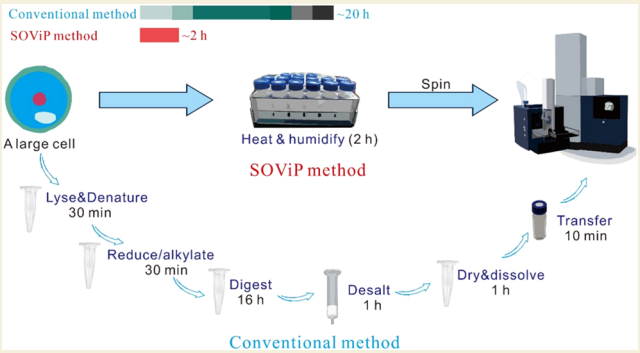

KEYWORDS: *single-cell proteomics, oocyte aging, LC-MS, sample preparation, machine learning*

INTRODUCTION

Single-cell analysis has become a key technology to elucidate cellular heterogeneity and dynamic functions.[1,2] Techniques such as single-cell DNA sequencing (scDNA-seq) and single-cell RNA sequencing (scRNA-seq) are relatively mature and have been widely applied. However, genomics and transcriptomics provide only indirect insights into cellular states. Proteins are the workhorse for virtually all cellular processes, but the levels of protein and mRNA are only moderately correlated.[3,4] Therefore, single-cell proteomics (scProteomics) is an indispensable tool for elucidating the intricacies of cellular heterogeneity at the phenotype level. Unlike DNA and RNA whose signals can be amplified by robust polymerase chain reaction-based methods, scProteomics is still technically challenging, since no comparable amplification methods currently exist for proteins. Some pioneering papers have been published using capillary electrophoresis (CE) or microfluidic devices for scProteomics, including CE-MS detection for early stage frog embryo cells[5,6] in 2016, nanoliter-scale oil-air-droplet (OAD) chip,[7] and nanodroplet processing in one-pot for trace samples (nanoPOTS)[8] for single somatic cells in 2018.

Due to advances in sample preparation and mass spectrometric instrumentation, a few studies have achieved proteomics profiling of single mouse oocytes or early embryos in the recent two years. Li et al. established an efficient and simplified single-cell proteomics (ES-SCP) workflow to realize proteomics profiling at the single-oocyte level.[9] In the ES-SCP workflow, oocytes were lysed through sonication and then heated for 15 min at 90 °C in a metal bath to denature proteins. After being cooled to room temperature, proteins were digested at 37 °C overnight and desalted with a C18 stage tip. Li et al. quantified more than 4000 protein groups from a pool of only 15 oocytes and more than 1500 protein groups from single oocytes. Huang et al. compared aged and young mouse and human oocytes using multiomics analysis.[10] Oocytes were sonicated three times in a lysis buffer containing 8 M urea and then centrifuged to remove

Received: March 5, 2025
Revised: April 23, 2025
Accepted: April 24, 2025
Published: May 1, 2025

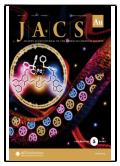

https://doi.org/10.1021/jacsau.5c00244
JACS Au 2025, 5, 2321−2333

remaining debris. Next, the collected supernatant was reduced, alkylated, digested by trypsin, and then desalted using a C18 solid phase extraction (SPE) column. Approximately 1100 protein groups were identified from single mouse oocytes, whereas nearly 10,000 genes were detected via scRNaseq. Very recently, Ye et al. developed One-Tip method, identifying ∼5400 proteins from single zygotes by narrow-window data-independent acquisition (nDIA) analysis with the current state-of-the-art mass spectrometer Orbitrap Astral.[11] The One-Tip sample preparation workflow consisted of eight steps, including multiple manual centrifugation steps. Additionally, the One-Tip method relied on specialized equipment and consumables such as Evosep and Evo-tips, which may limit its broader applicability.

In addition, single-cell multiomics of mouse oocytes have been reported. Jiang et al. developed a single-cell simultaneous transcriptome and proteome (scSTAP) analysis platform based on microfluidics.[12] Single oocytes were prelysed by Lys-C solution and then lysed by RapiGest. After the cell lysis, cell lyses were split into two aliquots: one for transcriptome analysis and the other for proteomic analysis. On average, 2663 protein groups and 19,948 genes were quantified from single mouse oocytes. He et al. developed an on-capillary alkylation microreactor (OCAM) to enable simultaneous proteome and metabolome profiling from the same cell.[13] In OCAM, proteins were first covalently bound to an iodoacetic acid functionalized open-tubular capillary microreactor, and metabolites were eluted before on-column digestion of captured proteins. An average of 2944, 3039, and 3085 proteins were quantified from single oocytes at GV (germinal vesicle), GVBD (germinal vesicle breakdown), and MII (metaphase II) stages, respectively, along with a total of 171 metabolites.

All of the above-mentioned methods require laborious, multistep operations for sample pretreatment of single oocytes or early embryos, and a simple and robust method is still lacking to minimize variations introduced at each step. Herein, we reason that the routinely applied sonication, desalting, and acidification steps can be omitted and thus developed a simple one-step vial-based pretreatment (SOViP) for deep scProteomics of manually picked single germline cells. In SOViP, we integrated all of the sample preparation steps into a single incubation step to realize lysis and digestion simultaneously. The hands-on time is merely a few minutes for a single cell, and the samples are ready for nanoLC-MS/MS analysis immediately after incubation. To avoid cross-contamination and sample loss, we replaced the widely used 384-well plates with autosampler vials. To ensure accessibility and low cost, we demonstrated that the incubation could be performed in a thermostated water bath. In addition, tens to hundreds of samples can be processed in a single batch, enabling SOViP a robust, simple, and high-throughput method for broad applications.

Infertility is estimated to affect 8−12% of reproductive-aged couples worldwide, with declining fertility being one of the leading causes.[14,15] Reduced oocyte quality due to aging is one of the most critical factors impacting female fertility. Single oocytes are heterogeneous and dynamic; however, proteomics studies at the single-cell level for oocyte aging are still scarce. The mechanisms underlying oocyte aging are still incompletely unraveled. To facilitate oocyte aging studies, we applied SOViP to profile mouse oocytes at different ages herein. On average, over 6500 protein groups can be quantified from single oocytes. To the best of our knowledge, this study represents the first scProteomics investigation of oocyte aging with deep coverage, providing a valuable resource for understanding oocyte quality and female fertility.

EXPERIMENTAL SECTION

Collection of Single Mouse Oocytes

All animal protocols were carried out in accordance with the rules and guidelines of the Medical Ethical Committee of the Beijing Institute of Lifeomics. Female mice of various ages, all on a C57BL/6 background, were raised under specific pathogen-free (SPF) conditions in individually ventilated cages.

To collect oocytes at GV stages, female mice at different ages were intraperitoneally injected with 5 IU of pregnant mare serum gonadotrophin (PMSG). The intact ovaries were taken after 48 h, and their surfaces were punctured with needles to release the oocytes. Granule cells were carefully removed by gently pipetting oocytes repeatedly in a prewarmed M2 medium. Next, the oocytes were individually isolated and collected using a mouth pipet with an internal diameter slightly larger than that of the oocyte under a stereoscopic microscope (Nikon SMZ18, Japan). To ensure that only one oocyte is transferred at a time, each oocyte was placed in a drop of PBS and gently moved by the mouth pipet.

Proteomics Sample Preparation

Single, clean oocytes collected from the above steps were transferred into 3 μL of the master mix at the bottom of 384-well plates (Eppendorf, Protein LoBind, Order No. 0030624300) or autosampler vials (Waters, QuanRecovery). The remaining liquid in the pipet was expelled repeatedly to ensure the oocyte was successfully transferred into the master mix of sampler vials or 384-well plates, with all steps performed under the stereomicroscope. The success rate of collecting single oocytes is nearly 100%. Note, we recommend a control liquid volume less than 3 μL for each oocyte transfer. The master mix contained 0.2% *n*-Dodecyl-*β*-D-Maltoside (DDM), 100 mM N-2-hydroxyethylpiperazine-N-2-ethanesulfonic acid (HEPES), and 20 ng/μL sequencing grade modified Trypsin (Promega). After being sealed with self-adhesive sealing films or screw caps, 384-well plates and autosampler vials were incubated at 37.0 °C in a commercial cellenONE system (85% humidity) or a thermostat water bath.

Human embryonic kidney (HEK) 293T cells were cultured in Dulbecco's Modified Eagle Medium (DMEM) supplemented with 10% (v/v) fetal bovine serum (FBS) and Penicillin/Streptomycin (1:1000) at 37 °C in a 5% CO_2 atmosphere. Subsequently, 293T cells were detached using trypsin treatment and underwent thorough washing with phosphate buffered saline (PBS) three times. Then, lysis buffer was added, and the lysis was assisted by noncontact sonication. The composition of the lysis buffer included 40 mM HEPES (pH 7.5), 300 mM NaCl, 1.2 M guanidine HCl, 2% (w/v) DDM, and a protease inhibitor mixture. Protein concentration was measured by a NanoDrop One. Different amounts of 293T cell lysates were added into 3 μL of the master mix at the bottom of 384-well plates or autosampler vials and then incubated as described above.

All samples were kept at −80 °C prior to nanoLC-MS analysis. The sealing films of 384-well plates or the caps of the vials were cleaned before injection. Note, no desalting or acidification steps were included in this protocol.

RESULTS AND DISCUSSION

Design of the SOViP Strategy

In scProteomics, it is well-known that reducing reactor volume minimizes contact surfaces, thereby decreasing sample loss due to nonspecific binding to reactor surfaces.[16] Consequently, successful scProteomics for somatic cells are predominantly achieved using various microfluidic platforms with nanoliter-scale microreactors, such as oil-air-droplet (OAD) chip,[7] nanodroplet processing in one-pot for trace samples (nanoPOTS),[8,17] sequential operation droplet array (SODA) system,[18] nested nanoPOTS (N2) chip,[19] and BOXmini

https://doi.org/10.1021/jacsau.5c00244
JACS Au 2025, 5, 2321−2333

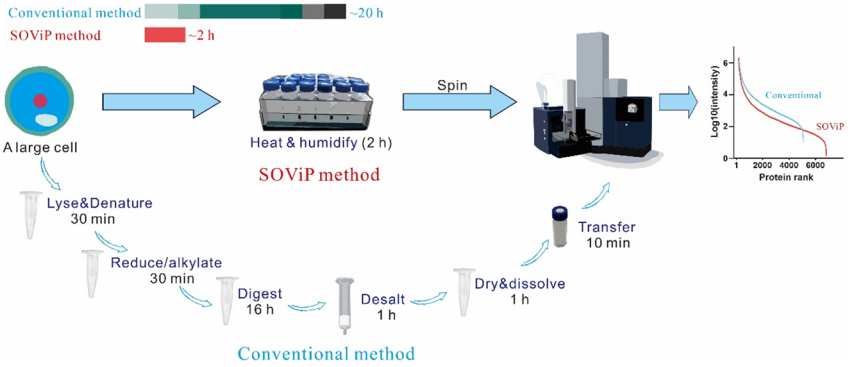

Figure 1. Scheme for the comparison of the simple one-step vial-based pretreatment (SOViP) method with a conventional multistep method.

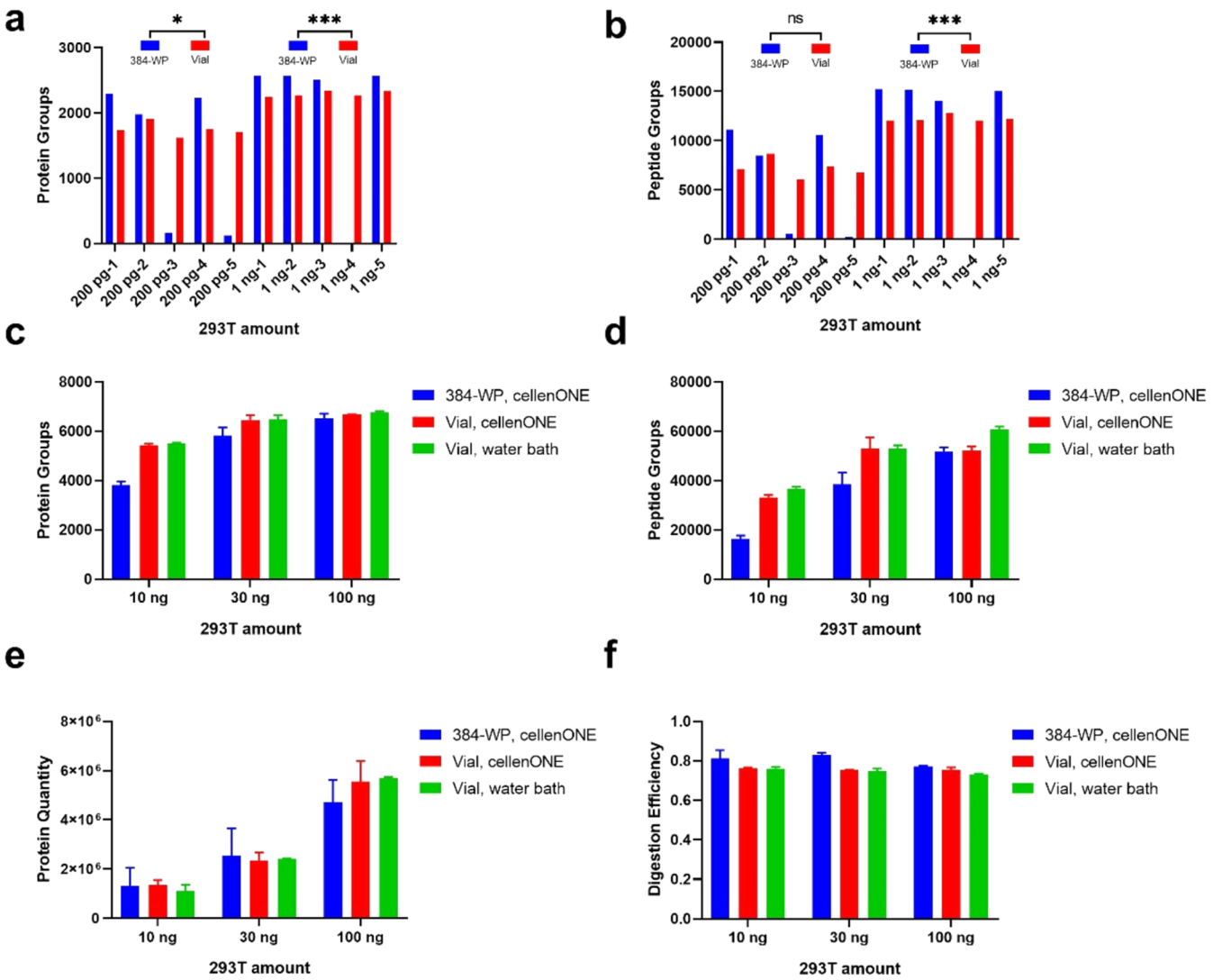

Figure 2. Comparison of 384-well plate and autosampler vial for processing different amounts of 293T cell lysate. (a, b) Number of protein groups (a) and peptide groups (b) identified from 200 pg and 1 ng of 293T cell lysate using a 384-well plate or vials. Analyses were conducted using a two-tailed unpaired Student's *t* test (***$p < 0.001$, *$p < 0.05$, ns: not significant) after excluding failed samples. (c, d) Number of protein groups (c) and peptide groups (d) identified from 10, 30, and 100 ng of 293T cell lysate using a 384-well plate or vials in a cellenONE or a water bath. (e, f) Comparison of protein quantity (e) and digestion efficiency (f) for 10, 30, and 100 ng of 293T cell lysate processed using a 384-well plate or vials in a cellenONE or a water bath. "384-WP" and "Vial" indicate 384-well plate and autosampler vial, respectively.

SCP.[20] Alternatively, 1536-well plates[21] and 384-well plates[22] integrated with the cellenONE system have also been reported.

Oocytes and early embryos are much larger than somatic cells, containing 100 times more protein (~20 ng for mouse oocytes and ~100 ng for human oocytes) than somatic cells (~200 pg). In addition, unlike somatic cells, which are often sorted in large numbers by a fluorescence-activated cell sorter or cellenONE, oocytes and early embryos are limited in number and are

https://doi.org/10.1021/jacsau.5c00244
JACS Au 2025, 5, 2321−2333

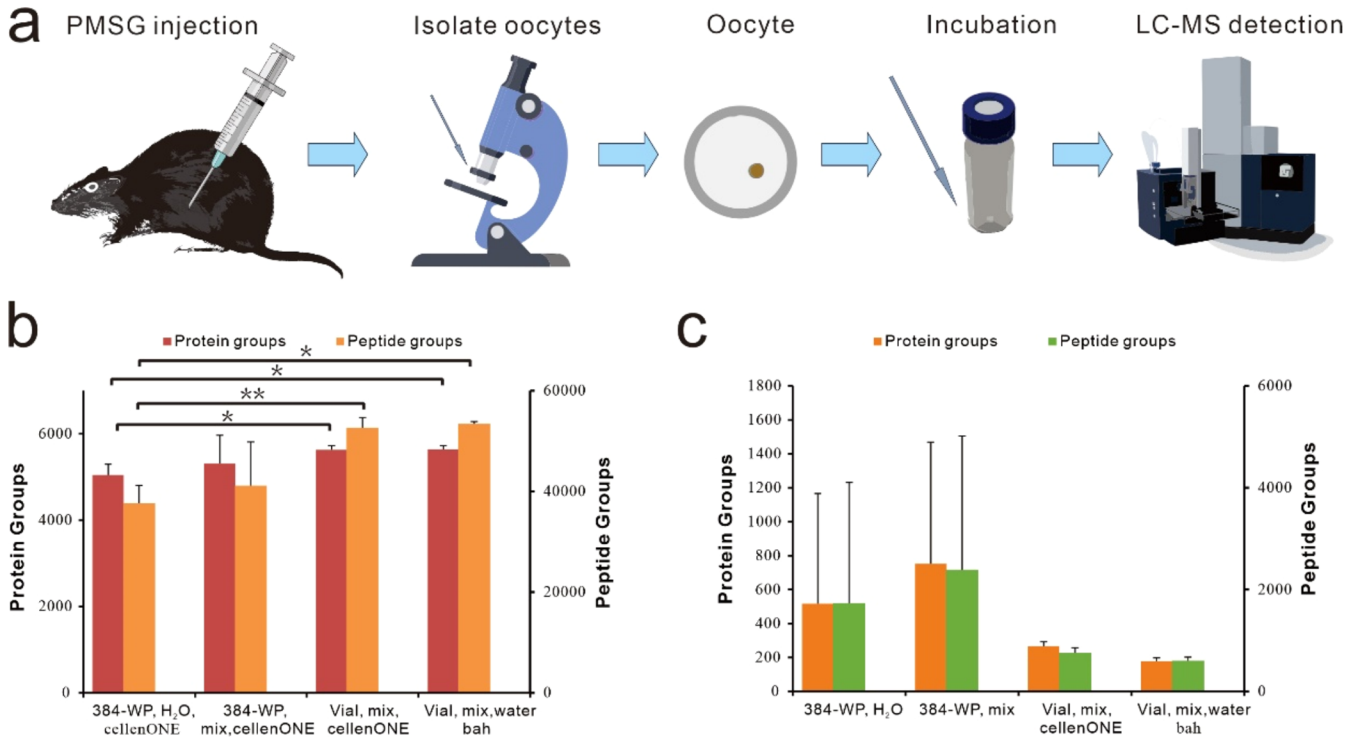

Figure 3. Method development for processing single mouse oocytes. (a) Workflow for processing single mouse oocytes using SOViP. (b) Comparison of the number of protein groups and peptide groups identified from single mouse oocytes using four protocols: Single mouse oocytes were kept in H_2O, transferred to a 384-well plate, freeze-dried, and incubated with 3 μL of the master mix in cellenONE ("384-WP, H_2O" group); or directly transferred into 3 μL of the master mix in a 384-well plate ("384-WP, mix" group). Alternatively, single mouse oocytes were transferred into 3 μL of the master mix in vials and then incubated in either cellenONE ("Vial, mix, cellenONE" group) or a water bath ("Vial, mix, water bath" group). Analyses were conducted using a two-tailed unpaired Student's *t* test (**$p < 0.01$, *$p < 0.05$.). (c) Comparison of the number of protein groups and peptide groups identified from blank controls using the above four protocols.

typically manually picked under a stereomicroscope or fluorescence microscope. Thus, their sample reactors do not need to be integrated with cell sorters. Though 384-well plates are compatible with direct injection into some liquid chromatography systems, the inadequate leakproofness of adhesive sealers and the remaining adhesive on sealers often cause problems (this will be detailed later). With the ultrahigh sensitivity of state-of-the-art MS instruments, such as timsTOF SCP, Orbitrap Astral, and timsTOF Ultra 2, a 10 ng injection is sufficient to achieve good proteome coverage. We hypothesize that the slightly higher sample loss associated with larger reactors may not significantly compromise results in this context. Thus, autosampler vials with superior leakproofing are chosen as reactors for oocytes in this study. In addition, 384-well plates require incubation in a cellenONE system, which supplies a controlled temperature and high-humidity water vapor generated from ultrapure water. Whereas for autosampler vials with robust leakproofness, routinely used thermostatic water baths may serve as their incubation chamber. Moreover, sample preparation should involve minimal steps to reduce the time and variability.

To make it as simple and stable as possible, we developed the SOViP method, which integrated all of the sample pretreatment steps into a single step using ready-to-inject autosampler vials (Figure 1). The routinely required steps, including sonication, heating, cooling, reduction, alkylation, desalting, vacuum dryness, reconstitution, and acidification, were omitted in our protocol. Instead, a single incubation step for simultaneous lysis and digestion remains in SOViP, ensuring the operation is as simple as possible.

Consequently, the SOViP method has several merits:

(1) Easy and fast sample preparation: The only manual step involves placing single oocytes into the master mix at the bottom of autosampler vials, followed by a ∼2-h incubation. Tens to hundreds of single cells can be processed per batch, with only a few minutes of hands-on time per cell.

(2) Prevention of contamination and cross-contamination: Unlike 384-well plates or open-ended microfluidic chips, autosampler vials can be tightly sealed with screw caps, ensuring excellent leakproofness.

(3) Improved injection completeness: Autosampler vials are better suited for injection needles than most 384-well plates, where incomplete injection is common.

(4) ∼100% success rates with reduced variability: The adhesive from adhesive sealers can easily block injection needles/injection ports/plungers, resulting in incomplete injections or even failures. Meanwhile, the adhesive also increases the frequency of LC system maintenance, which prolongs instrument downtime.

(5) Simpler operation: When using 384-well plates, unused wells must be sealed and resealed multiple times during preparation, adding complexity. Autosampler vials eliminated this need.

(6) Flexibility to incorporate sonication: Noncontact sonication can be employed to enhance lysis for certain sample types.

(7) Extended sample storage: Samples in 384-well plates must be injected within ∼2 days due to evaporation, while those in autosampler vials remain stable for ∼2 weeks.

https://doi.org/10.1021/jacsau.5c00244
JACS Au 2025, 5, 2321−2333

(8) Cost efficiency: The cellenONE system is expensive and accessible in only a few laboratories, whereas most laboratories already have a thermostatic water bath.

Evaluation of SOViP for Cell Lysate Samples

We first compared the performance of 384-well plates vs autosampler vials with 200 pg and 1 ng of 293T cell lysate (Figure 2a,b), amounts close to the protein amount in a single somatic cell. Out of the total ten tested samples, three failed in the 384-well plate group, whereas all samples yielded stable results in the autosampler vial group. This highlighted the superior stability afforded by using autosampler vials over 384-well plates. Nevertheless, excluding the failed injections (three data with less than 200 protein groups identified), 21 and 11% more protein groups were identified using 384-well plates compared to autosampler vials for 200 pg (2168 vs 1799) and 1 ng (2554 vs 2297) of 293T cell lysate, respectively; Meanwhile, 384-well plates led to 30 and 20% more peptide groups identified for 200 pg (10,056 vs 7727) and 1 ng (14,880 vs 12,290) of 293T cell lysate, respectively. This is rational, as the reactor volume of 384-well plates is smaller than that of autosampler vials, leading to less sample loss caused by nonspecific binding. Consequently, 200 pg benefit more than 1 ng from smaller reactor volume in our results.

Next, we compared these two reactors for higher protein amounts and obtained different outcomes. 10, 30, and 100 ng of 293T cell lysate span the protein range of mouse to human oocytes at various stages. As shown in Figure 2c,d, the 384-well plate group still showed significantly higher variability than the autosampler vial group in terms of protein groups, peptide groups, protein quantity, and digestion efficiency. For 10−100 ng of 293T cell lysate, more protein groups and peptide groups were identified using autosampler vials, in contrast to the results for 200 pg and 1 ng. This indicates that sample loss due to nonspecific binding is minimal for high protein samples, while sample loss due to evaporation during incubation is more significant when sealing is inadequate. When using autosampler vials, 5014 ± 49 protein groups were identified from 10 ng of 293T cell lysate, and this number increased to 5714 ± 29 and 6113 ± 14 for 30 and 100 ng of 293T cell lysate, respectively. Not surprising, variation decreased along with increasing protein amount. In addition, digestion efficiency, represented by the relative percentage of fully tryptic peptides to all identified peptides, achieved close to 80% (Figure 2f), which is satisfactory for a simple one-step and one-pot sample pretreatment.

Lastly, to enhance accessibility, we tested using a thermostatic water bath to replace cellenONE when using autosampler vials. A thermostatic water bath can supply stable temperature and high humidity, although not as precisely controlled as cellenONE. Moreover, the water vapor in thermostatic water is not clean, requiring that the reactor be well sealed. Encouragingly, the water bath achieved results similar to those of cellenONE, with no significant differences in protein groups, peptide groups, protein quantity, or digestion efficiency between the water bath group and the cellenONE group. Importantly, both the water bath group and the cellenONE group demonstrated high quantification accuracy by comparing protein group intensities from 10, 30, and 100 ng of the 293T cell lysate (Figure S1). In addition, no significant variation was observed in peptide samples, whether acidified or not, across Day 0, Day 3, and Day 5 (Figure S2), supporting the exclusion of the acidification step in SOViP.

Development of SOViP for Mouse Oocytes

The SOViP protocol for mouse oocytes is depicted in Figure 3a. Female mice were intraperitoneally injected with PMSG to accelerate the follicular development. Granule cells were carefully removed, and single oocytes were isolated and collected under a stereoscopic microscope. Single oocytes were directly transferred to the bottom of autosampler vials using mouth pipet. After a 2 h incubation, the samples in the autosampler vials were directly injected. The workflow is simple and straightforward (Figure 3a).

During workflow optimization, we compared four protocols for single mouse oocytes: (1) Oocytes were kept in H_2O, transferred to a 384-well plate, freeze-dried, and then incubated in cellenONE after adding the master mix ("384-WP, H_2O" group); (2) Oocytes were directly transferred into the master mix in a 384-well plate and then incubated in cellenONE ("384-WP, mix" group); (3) Oocytes were directly transferred into the master mix in autosampler vials and then incubated in cellenONE ("Vial, mix, cellenONE" group); and (4) Oocytes were directly transferred into the master mix in autosampler vials and then incubated in a water bath ("Vial, mix, water bath" group). The "384-WP, H_2O" group involved additional transfer and freeze-drying steps but yielded the lowest numbers of identified protein and peptide groups (Figure 3b). Direct transfer into 384-well plates without freeze-drying yielded slightly higher protein and peptide group counts (Figure 3b). In contrast, the two autosampler vial groups, whether using cellenONE or a water bath, produced significantly higher protein and peptide group counts than those of either of the 384-well plate groups (Figure 3b). Moreover, the autosampler vial groups exhibited much lower variability compared with the 384-well plate groups, consistent with the trend observed for cell lysates (Figure 2).

To assess background contamination, we compared blank controls for those four protocols as well (Figure 3c). When using 384-well plates, approximately 600 protein groups with large variations were detected. In contrast, merely ∼200 protein groups were detected in the two autosampler vial groups, likely originating from reagent and environmental background noise.[12] Overall, the autosampler vial-based protocols demonstrated clear advantages over the 384-well plate-based protocols for pretreating mouse oocytes.

Application of SOViP in Oocyte Aging

Aging exerts multifaceted effects on the female reproductive system, with a notable decline in oocyte quality and an impediment to embryo developmental potential.[14] In 2023, Isola et al. built a single-cell RNA sequencing atlas of the aging mouse ovary by comparing ovarian tissues from 3-month-old and 9-month-old mice.[23] This study provided a comprehensive cellular map of the transcriptomic changes in the aging mouse ovary, revealing a doubling of immune cell populations in aged ovaries. Huang et al. performed scProteomics, translatomics, and transcriptomics analysis on GV-stage oocytes from aged and young mice and humans.[10] Huang et al. identified a crucial m6A-containing YTHDF3-binding target Hells and highlighted cross-species conservations and differences between aged mouse and human oocytes. Despite significant strides in research, the intricate mechanisms governing oocyte senescence remain incompletely elucidated, and effective approaches to improve oocyte quality are still lacking.[24]

Naturally aged female mice are widely used as in vivo models for oocyte aging studies because they exhibit physiological

https://doi.org/10.1021/jacsau.5c00244
JACS Au 2025, 5, 2321−2333

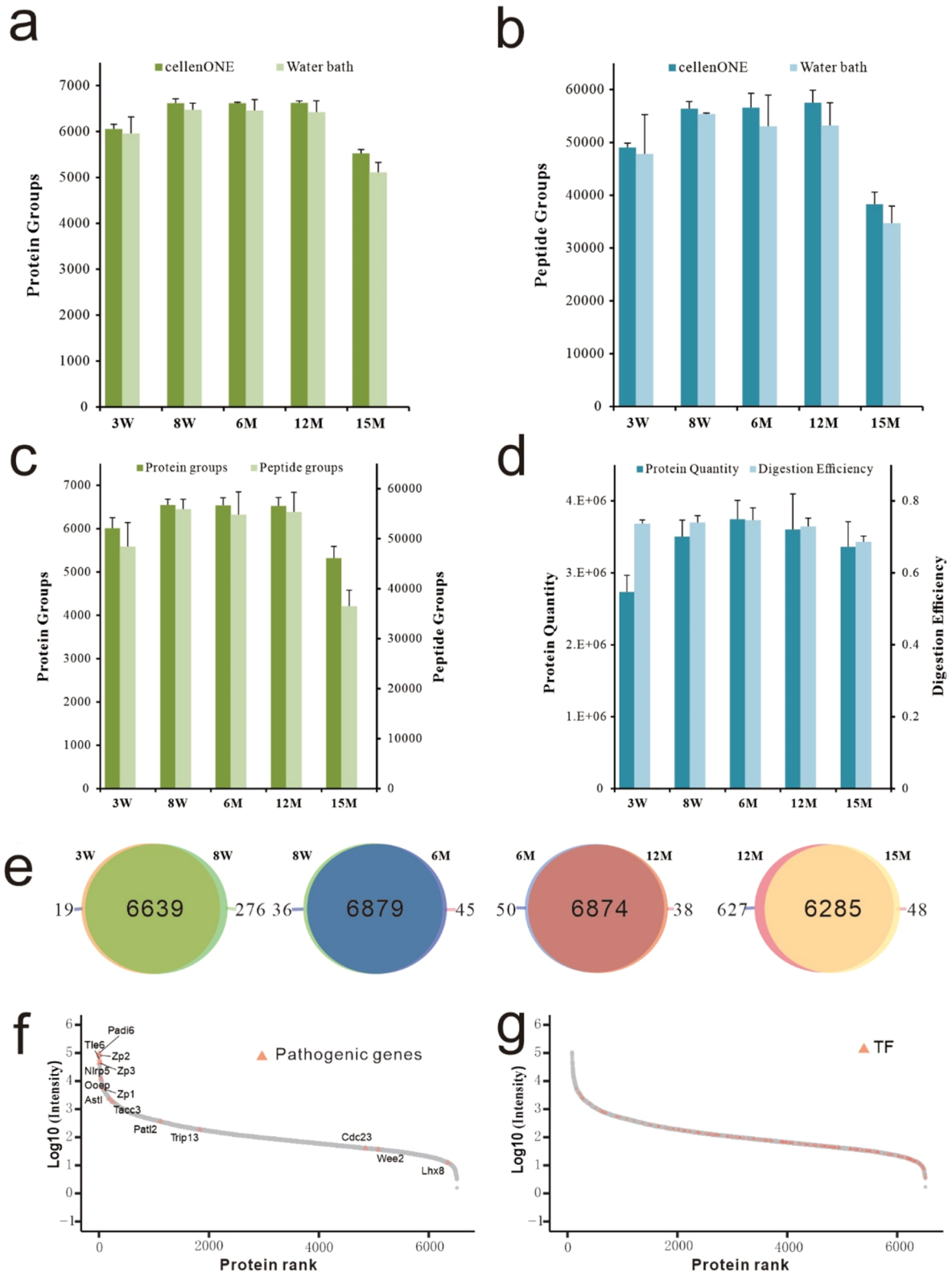

Figure 4. Application of SOViP to oocyte aging. (a, b) Comparison of the number of protein groups (a) and peptide groups (b) identified from single mouse oocytes at five ages incubated in cellenONE or a water bath. (c) Number of protein groups and peptide groups identified from single mouse oocytes at five ages. (d) Comparison of protein quantity and digestion efficiency for single mouse oocytes at five ages. (e) Venn diagrams showing the overlap of identified protein groups across four adjacent age groups. (f, g) Assessment of dynamic range based on protein abundance rank (mean values for the five age groups) and annotation of 198 mouse transcriptional factors (f) and 21 reported pathogenic genes involved in human oocyte and early embryo development (g). 3W, 8W, 6M, 12M, and 15M represent 3-week, 8-week, 6-month, 12-month, and 15-month samples, respectively.

changes that resemble those of menopausal women, including irregular oestrus cycles. C57BL/6 mice, commonly used for such studies, are weaned at 3−4 weeks after birth and attain sexual maturity at 8−12 weeks of age.[25] Studies have shown that the

https://doi.org/10.1021/jacsau.5c00244
JACS Au 2025, 5, 2321−2333

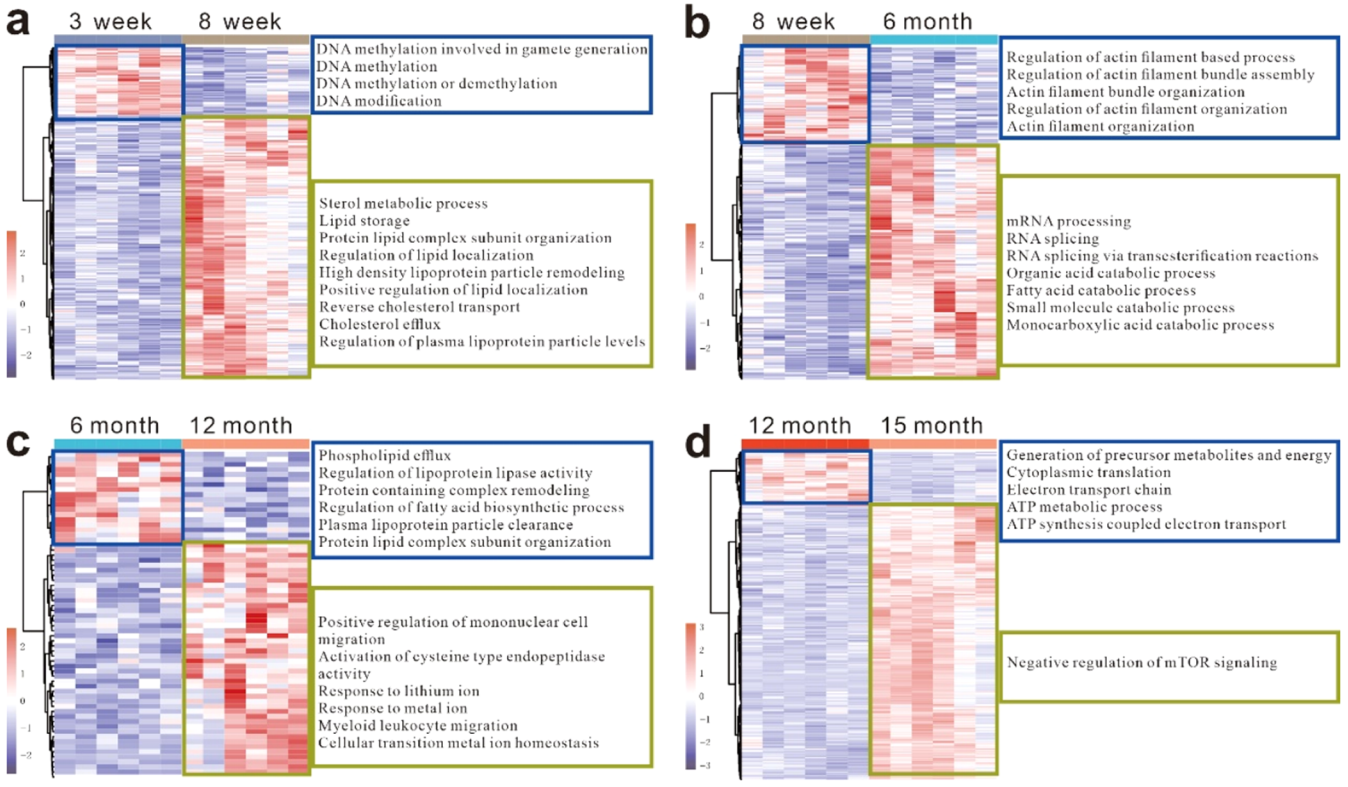

Figure 5. Oocyte characteristics across different ages. (a–d) Left: Unsupervised hierarchical clustering of proteins showing significant regulation ($p < 0.05$, one-sided ANOVA) and FC > 1.5 fold in each adjacent age groups: 3 weeks vs 8 weeks (a), 8 weeks vs 6 months (b), 6 months vs 12 months (c), and 12 months vs 15 months (d). Right: Gene ontology biological processes enrichment analysis of the protein clusters from the heatmap. Number of biological replicates: $n = 6$ for all age groups.

fertility of C57BL/6 female mice begins to decline from the highest level at approximately 6 months of age and drops markedly by 12 months.[24] By 15 months, fertility is nearly exhausted,[25] when ovulated oocyte numbers largely diminish and oocyte quality decays. To comprehensively study reproductive senescence, we selected five age groups of wild-type female mice: 3 weeks (postweaning), 8 weeks (adult), 6 months (midlife), 12 months (late reproductive life), and 15 months (end of fertility).

Using the developed SOViP workflow, we conducted scProteomics analysis to deeply profile the proteomes of mouse oocytes at the GV stage and investigate reproductive aging at the single-cell level. We achieved deep proteome profiling of single mouse oocytes from weaning to fertility end period, using both cellenONE and water bath (Figure 4 and Table S2). Results from the two methods were highly similar, with cellenONE yielding only slightly higher numbers of identified protein and peptide groups (Figure 4a,b), consistent with previous findings (Figure 3). Principal component analysis (PCA) and Pearson correlation coefficients demonstrated strong concordance between biological replicates and high correlation between the two preparation methods (Figure S3). Across the five age groups, proteomic analysis revealed dynamic patterns. On average, 6009 protein groups were identified from single oocytes at 3 weeks, increasing significantly to over 6500 in the 8-week to 12-month groups before declining sharply to ~5300 at 15 months, corresponding to the poor quality of oocytes at the end of fertility (Figure 4c). A similar trend was observed for the peptide group counts. This rise-and-fall pattern suggests that the expression of approximately 500 fertility-related genes is low at 3 weeks and that over 1000 genes are downregulated at 15 months (Figure 4c,e). Noteworthily, the total protein quantity increased steadily from 3 weeks to 6 months but declined from 6 to 15 months (Figure 4d), indicating age-dependent differences in protein expression patterns. A high proportion of protein groups were shared between adjacent age groups (Figure 4e), with 6139 protein groups coidentified across all five age groups (Figure S4), indicating most proteins continuously expressed from 3 weeks to 15 months. Remarkably, using the easy-to-use one-step SOViP protocol, we achieved dynamic ranges of quantified protein groups spanning 6 orders of magnitude (Figure S5), capturing a high ratio of low-abundance proteins. Among them, 14 of the 36 reported pathogenic genes involved in human oocyte and early embryo development[26] were quantified and marked in Figure 4f. Additionally, we quantified 191 mouse transcription factors across a wide dynamic range (Figure 4g and Table S1).

Overall, a total of 6983 protein groups were identified and 6927 protein groups were quantified from single mouse oocytes (Table S2). On average, ~6500 protein groups were quantified from single oocytes aged 8 weeks to 12 months. Notably, detecting over 5500 protein groups from a single mouse oocyte has not been reported previously, even using more advanced MS like Orbitrap Astral or timsTOF Ultra 2 combined with multistep protocols.[11] Therefore, our simple one-step method represents a significant technical advancement in the pretreatment of single oocytes. Moreover, the five age groups from 3 weeks to 15 months provide a comprehensive single-cell proteomic resource for age-related fertility research.

https://doi.org/10.1021/jacsau.5c00244
JACS Au 2025, 5, 2321−2333

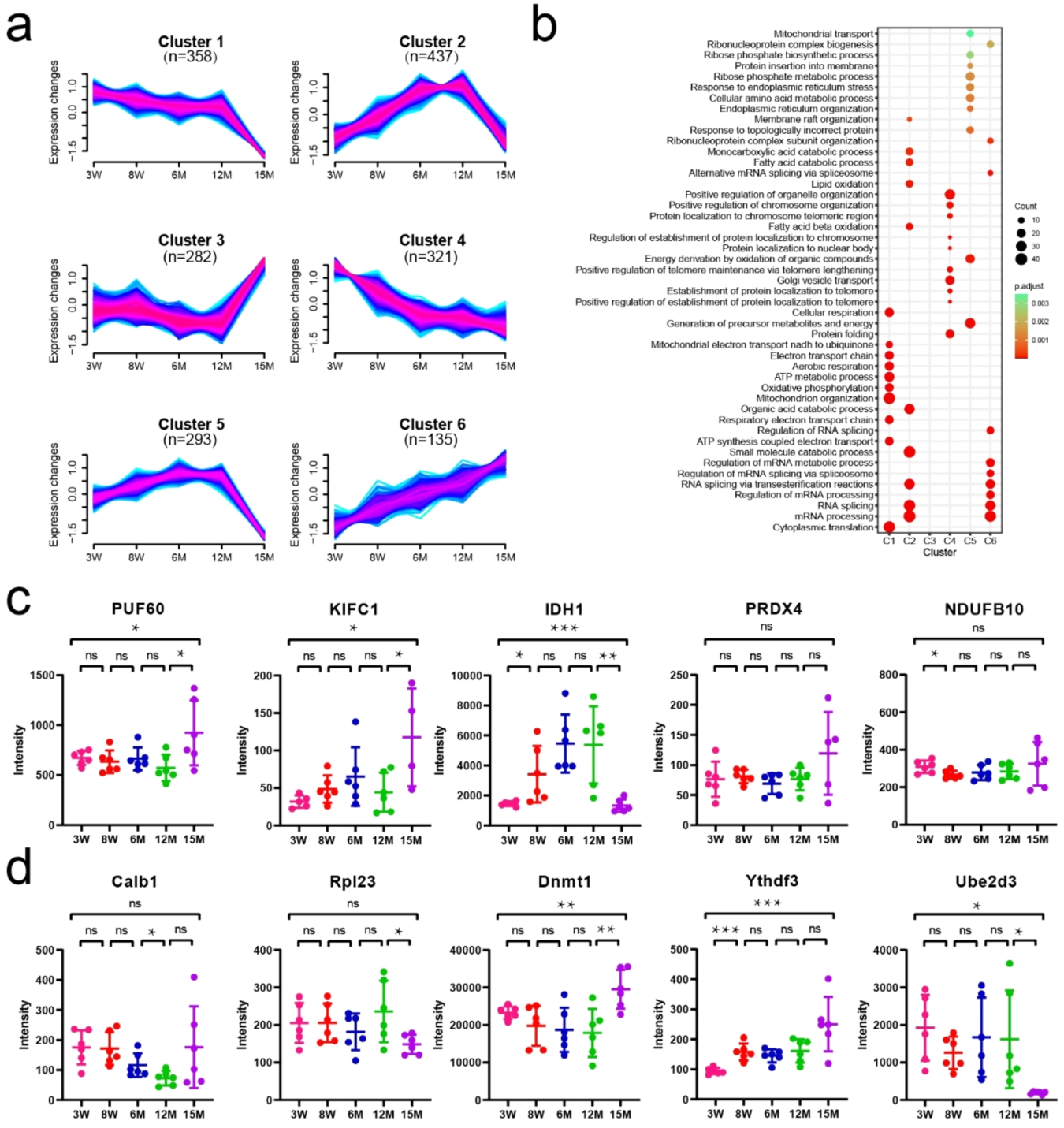

Figure 6. Biological insights into mouse oocyte aging. (a) Dynamic proteins were categorized into six clusters using Mfuzz soft clustering. A total of 3203 dynamic proteins filtered by an ANOVA p-value <0.05 were analyzed. Proteins were considered significant regulation across five groups if they presented a Benjamini−Hochberg (B−H) adjusted p-value of less than 0.05 from one-sided ANOVA. (b) Representative biological processes from gene ontology (GO) enrichment analysis for each cluster are displayed. Dot size indicates the number of enriched proteins for each GO term, and the color scale represents the statistical significance of each enrichment. (c) Relative expression of five reported marker proteins related to fertility at different ages ($n = 6$). (d) Relative expression of five reported oocyte markers. Data are presented as mean ± SD. Analyses were conducted using a two-tailed unpaired Student's t test (***$p < 0.001$, **$p < 0.01$, *$p < 0.05$, ns: not significant); 3W, 8W, 6M, 12M, and 15M indicate 3-week, 8-week, 6-month, 12-month, and 15-month samples, respectively.

Oocyte Characteristics in Different Ages

To investigate biological characteristics for oocytes at different ages from scProteomics data, we then performed unsupervised hierarchical clustering of differentially expressed proteins. Data from the cellenONE group and the water bath group were combined for biological analysis, and comparisons between each pair of adjacent age groups are presented in Figure 5. All data were correctly clustered in corresponding age groups with representative biological processes (BPs) for each cluster highlighted in the boxes on the right. Gene ontology (GO)

https://doi.org/10.1021/jacsau.5c00244
JACS Au 2025, 5, 2321−2333

enrichment analysis of clusters revealed the unique characteristics of these age groups. DNA methylation involved in gamete generation, DNA methylation, DNA modification or demethylation, and DNA modification were enriched in 3-week oocytes, suggesting that 3-week oocytes in young mice immediately after weaning tend to complete essential developmental milestones and maintain viability. Regulations of lipid and lipoprotein, including lipid storage, protein lipid complex subunit organization, regulation of lipid localization, high density lipoprotein particle remodeling, positive regulation of lipid localization, and regulation of plasma lipoprotein particle levels, were enriched in 8-week oocytes, indicating that oocytes are extensively active at metabolizing lipids during the process of sexual maturation. When compared with 8-week oocytes, upregulation of proteins in 6-month oocytes mainly related to mRNA processing, RNA splicing, RNA splicing via transesterification reactions, organic acid catabolic process, fatty acid catabolic process, small molecule catabolic process, and monocarboxylic acid catabolic process, which shows the augmented RNA expression and catabolic processes in 6-month oocytes correlates with enhanced reproductive capability. For oocytes collected from 12-month-old mice, the upregulation of cysteine-type endopeptidase activity suggested an increase in apoptosis.[27] Additionally, the upregulation of proteins primarily associated with the migration of mononuclear cells and myeloid leukocytes were resulted from age-related senescence,[28,29] and the elevated responses to metal ions and the negative regulation of T-cell receptor and antigen receptor-mediated signaling pathways were also correlated with significant reproductive senescence. Meanwhile, the downregulation of fatty acid biosynthesis, lipoprotein lipase activity, and plasma lipoprotein particle clearance indicated abnormal lipid metabolism in oocyte senescence.[30,31] Oocytes collected from 12-month-old mice exhibited higher adenosine triphosphate (ATP) activity and electron transport, compared to 15-month-old oocytes, which were at the end of fertility, indicated the progressive impairment of mitochondrial function with age. In 15-month-old oocytes, negative regulation of mammalian target of rapamycin (mTOR) signaling was elevated, which need further investigation, as previous studies reported inconsistent conclusions in this regard.[32]

Biological Insights into Oocyte Aging

To identify the significantly enriched functional or regulatory features governing mouse oocyte aging across all of the five age groups, we grouped all of the significantly regulated 3203 protein groups into six clusters according to their expression patterns by means of Mfuzz algorithm (Figure 6a,b). Cluster 6 proteins (n = 135) showed a consecutively increasing trend. Cluster 6 proteins were enriched in mRNA and splicing activities, including alternative mRNA splicing via spliceosome, mRNA processing RNA splicing, regulation of mRNA processing, RNA splicing via transesterification reactions, regulation of mRNA splicing via spliceosome, and regulation of mRNA metabolic process. In contrast, Cluster 4 proteins (n = 321) displayed trends opposite to those of Cluster 6 proteins and were enriched in organelle organization, chromosome organization, and associated protein localization activities. Cluster 2 and Cluster 5 displayed similar rise-and-fall trends, with protein expression levels in both clusters decreasing sharply at 15 months. These proteins were primarily associated with energy-consumption-related GO categories. Proteins in Cluster 3 (n = 282) exhibited a gentle increase at 8 weeks, followed by a gradual decline from 8 weeks to 12 months, and a sharp surge at 15 months. However, no significant BPs were identified for Cluster 3 proteins. Collectively, these findings underscore the close links between age-related protein abundance dynamics and distinct BPs.

Next, we investigated the abundances of five previously reported protein markers related to aging and reproductive capacity across the five age groups (Figure 6c), since scProteomics provides novel insights compared to bulk proteomics and single-cell RNA sequencing. PUF60 (Poly(U) Binding Splicing Factor 60) was reported as a potential core splicing factor responsible for the decline of oocyte developmental potential in reproductively aging mice, based on the observation that the expression level of PUF60 progressively decreased with oocyte aging using tandem mass tag (TMT)-labeled bulk proteomics involving hundreds of oocytes.[24] However, in our scProteomics data, PUF60 remained stable from 3 weeks to 12 months before increasing at 15 months, suggesting that further research is required to elucidate its role in oocyte aging. Molecular motor KIFC1 (kinesin superfamily protein C1) was reported to be deficient in human oocytes, leading to spindle instability.[33] Similarly, KIFC1 depletion induced spindle instability in mouse oocytes. Nevertheless, in our data, KIFC1 levels did not decline with oocyte aging (Figure 6c), indicating that KIFC1 may not significantly contribute to the decline of reproductive capacity in mice. Additionally, three antioxidant genes (IDH1, PRDX4, and NDUFB10) have been reported to negatively correlate with age in human granulosa cells.[34] In our scProteomics data of mouse oocytes, however, only IDH1 was significantly downregulated in low-fertility ages (low at 3-week and undetected at 15-month), indicating potential conflicting expression levels between oocytes and granulosa cells. Figure 6d depicts the scProteomics results of five reported oocyte markers. Calb1 and Rpl23 were reported to be downregulated in MII-stage oocytes from aged (10−12 months) mice,[35] and our scProteomics results showed a similar downregulation pattern. DNMT1, which plays a critical role in the maintenance of DNA methylation during DNA replication, was reported to be significantly upregulated in aged mice (69−70 weeks).[36] Our scProteomics analysis confirmed this upregulation trend in GV-stage oocytes from aged mice. Ythdf3 has been shown to decrease markedly in aged mouse oocytes at the translational level while remaining unchanged at the mRNA level.[10] In contrast, our scProteomics data showed no significant difference from 8-week to 15-month-old oocytes. This discrepancy between translational and proteomic data may reflect post-translational modifications or protein degradation. UBE2D3 was reported to be upregulated in aged mice according to Western blot analysis, and this upregulation is responsible for age-related meiotic defects in oocytes.[37] In our scProteomics data of six individual oocytes, Ube2d3 was upregulated in two oocytes and downregulated in four; additional samples are needed for a statistically robust comparison. Notably, substantial variability was observed within the same age group, reflecting cellular heterogeneity and underscoring the necessity and value of single-cell studies. Overall, single-cell proteomic data can provide novel biologically meaningful insights into the mechanisms governing oocyte aging. Yet, our findings require further investigation and validation in future studies.

Machine Learning-Based Classification of Fertility Ability

Selecting high-quality oocytes is critical for assisted reproductive technologies such as in vitro maturation (IVM). Currently, no proteomics-based markers have been reported to accurately

https://doi.org/10.1021/jacsau.5c00244
JACS Au 2025, 5, 2321−2333

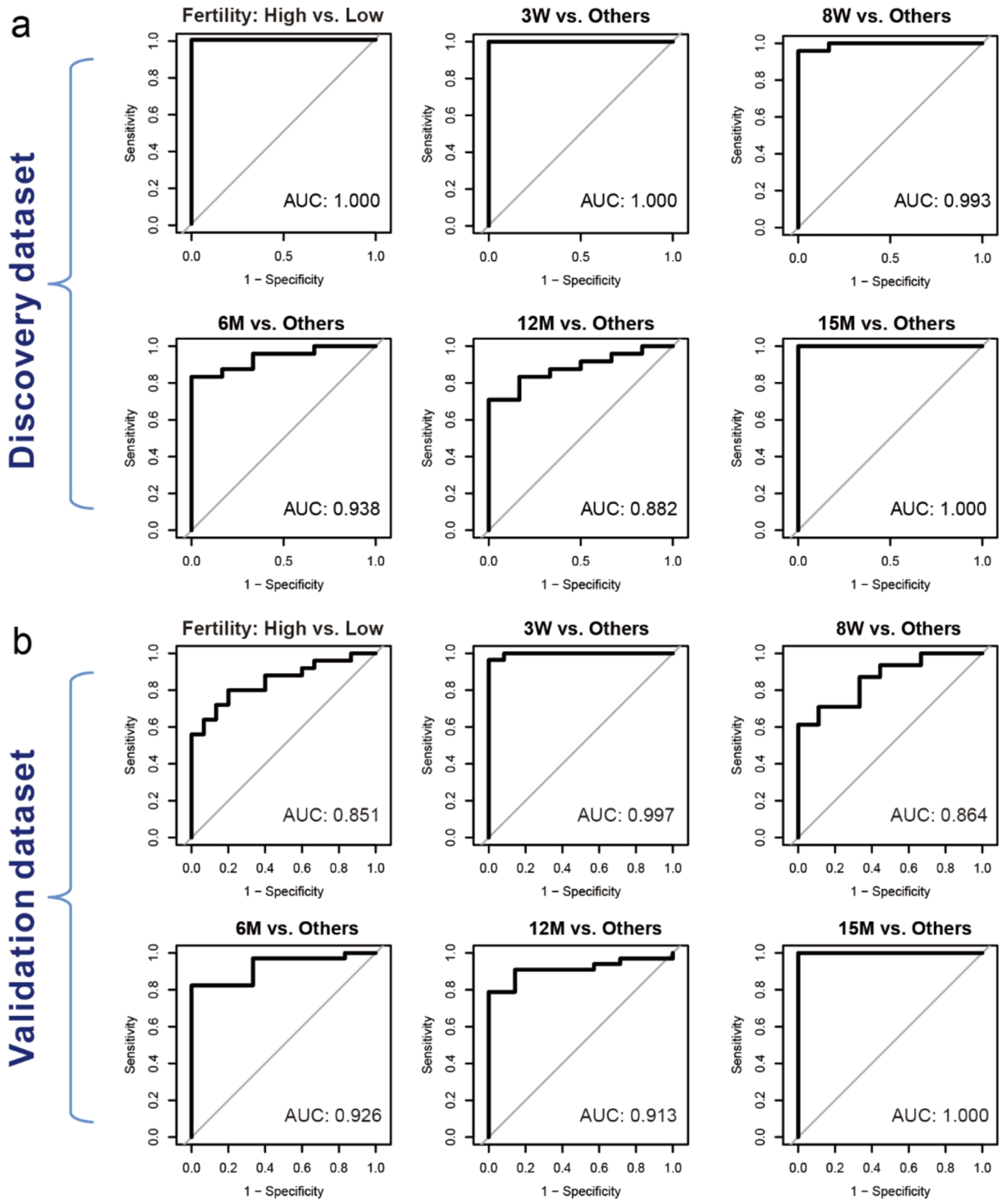

Figure 7. Classification of mouse oocyte aging and fertility level. (a) 10-fold cross validation area under the curve (AUC) value of the trained hybrid support vector machine (SVM)-random forest (RF) model for prediction of high versus low fertility. For training, the high fertility group included of 6M and 8W data, while 3W, 12W and 15M data formed the low-fertility group. The 10-fold cross validation AUC values of the trained hybrid SVM-RF model for predicting 3W, 8W, 6M, 12M and 15M against the corresponding rest groups, respectively. 3W, 8W, 6M, 12M, and 15M stand for 3-week, 8-week, 6-month, 12-month, and 15-month samples, respectively. (b) 10-fold cross validation AUC values of the generated classifier for prediction of high versus low fertility and for predicting 3W, 8W, 6M, 12M, and 15M against the corresponding rest groups in the validation data set.

https://doi.org/10.1021/jacsau.5c00244
JACS Au 2025, 5, 2321−2333

assess the age-associated reproductive potential of oocytes. To address this, we developed machine learning-based models to classify and differentiate the five age groups and their corresponding fertility levels using our scProteomics data. Because the sample size of this proof-of-concept study is limited, to alleviate overfitting, preliminary filtering of features by ANOVA or Lasso (Figure S6a) was performed. Then, SVM-RF hybrid models with cross validation were trained to generate the best classifiers to differentiate high (8W, 6M) versus low (3W, 12M, 15M) fertility ability. During the feature selection process, top 100 differentially expressed proteins (DEPs) selected from the 3203 dynamic proteins by ANOVA demonstrated excellent performance on both the discovery data set and validation data set (Figures S6b and 7), which is better than the Lasso-lambda_min set (Figure S6c−e) and the Lasso-lambda_1se set (Figure S6f−h) using the same discovery and validation data sets. The best classifier consisted of ten proteins, Cpsf6, Aldh16a1, Dctn3, Snx27, Rpl10, Cbx1, Oat, Atp5f1d, Fdx1, and Sra1, and achieved a high area under the curve (AUC) value of 1.000 in differentiating high versus low-fertility ability (Figure 7a). Importantly, those ten proteins can further accurately classify each of those five age groups and corresponding different fertility abilities as well. As shown in Figure 7a, the prediction accuracy achieved 1.000, 0.993, 0.938, 0.882, and 1.000 when classifying 3-week, 8-week, 6-month, 12-month, and 15-month against the rest groups, respectively. Protein expression levels and prediction probability of those ten proteins for five age groups are depicted in Figure S7. It is reasonable that the AUC value of 12-month is lower than the others since the fertility difference of 12-month is smaller than that of 3-week and 15-month. Furthermore, the reliability of those age and fertility biomarkers were validated in an independent data set (Table S3) comprising 40 single oocytes pretreated in cellenONE or in a water bath (n = 12 at 3W, n = 9 at 8W, n = 6 at 6M, n = 7 at 12M, n = 6 at 15M). Using the same workflow, those age and fertility biomarkers demonstrated accurate prediction as well, achieving an AUC value of 0.851 for discriminating high versus low-fertility ability and AUC values ranging from 0.864 to 1.000 for predicting the five age groups (Figure 7b). Our research laid a foundation for discovering age-specific biomarker panels associated with different fertility levels in future large-scale studies.

Though demonstrated with mouse oocytes, SOViP is applicable to other large cells and rare cell samples as well, including early embryos, follicles, granulosa cells, circulating tumor cells, etc. Importantly, since the SOViP protocol involves neither sample transfer nor impurity removal, metabolites are reserved, enabling direct application of single-cell proteome and metabolome dual-omics. As a result, SOViP can be used to study early embryonic development, folliculogenesis, infertility, and the maternal-to-zygotic transition in greater depth. Furthermore, automation of single-cell isolation and purification protocols, multiplexed labeling, and use of short gradients can be further developed to facilitate large-scale applications.

CONCLUSIONS

In summary, we developed an easy-to-use, one-pot method for the pretreatment of oocyte samples. The entire workflow is seamlessly integrated into a single step, enabling high throughput with minimal variation. Conventional "elution-drying-resuspension" procedures before LC-MS injection were omitted from our protocol to avoid sample loss and reduce processing time. To ensure high success rates, we replaced widely used 384-well plates with autosampler vials. Importantly, our method requires neither costly equipment or devices nor special reagents, and it can be easily automated and applied to other large cell types. Using this approach, we quantified over 6500 protein groups from single mouse oocytes and systematically compared their proteomic profiles from postweaning to end of fertility. This allowed us to identify unique molecular characteristics of oocytes at each age. Additionally, a classifier consisting of ten proteins demonstrated high discrimination power, accurately classifying all five age groups and corresponding fertility levels across the entire reproductive lifespan. The high reliability of this classifier was validated in an independent data set. To the best of our knowledge, this represents the largest single-cell proteomic data set for mouse oocyte aging to date. We anticipate that our strategy will facilitate widespread applications in proteomics-based embryogenesis, reproductive biology, and aging research at the single-cell level.

ASSOCIATED CONTENT

Data Availability Statement

The mass spectrometry proteomics data related to this study have been deposited to iProX[38] database (https://111.198.139.98/page/home.html) under the accession number IPX0010366000.

Supporting Information

The Supporting Information is available free of charge at https://pubs.acs.org/doi/10.1021/jacsau.5c00244.

Partial experimental section, partial results (Figures S1−S7) of method evaluation, and classifier performance comparison. (PDF)

Quantification information on 191 mouse transcriptional factors (Table S1). (XLSX)

Quantification proteins from single mouse oocytes at five age groups in discovery data set (Table S2). (XLSX)

Quantification proteins from single mouse oocytes at five age groups in validation data set (Table S3). (XLSX)

AUTHOR INFORMATION

Corresponding Authors

Fuchu He − *Department of Chemistry, College of Science, Southern University of Science and Technology, Shenzhen 518055, China; State Key Laboratory of Medical Proteomics, Beijing Proteome Research Center, National Center for Protein Sciences (Beijing), Beijing Institute of Lifeomics, Beijing 102206, China*; Email: hefc@nic.bmi.ac.cn

Yun Yang − *International Academy of Phronesis Medicine (Guang Dong), Guangzhou 510000, China*; orcid.org/0000-0003-0869-6498; Email: yangyunwww@126.com

Authors

Hui Zhang − *Department of Chemistry, College of Science, Southern University of Science and Technology, Shenzhen 518055, China; International Academy of Phronesis Medicine (Guang Dong), Guangzhou 510000, China*

Hailu Zhang − *State Key Laboratory of Medical Proteomics, Beijing Proteome Research Center, National Center for Protein Sciences (Beijing), Beijing Institute of Lifeomics, Beijing 102206, China*

Chuanxi Huang − *International Academy of Phronesis Medicine (Guang Dong), Guangzhou 510000, China*

https://doi.org/10.1021/jacsau.5c00244
JACS Au 2025, 5, 2321−2333

Qing Zeng − *International Academy of Phronesis Medicine (Guang Dong), Guangzhou 510000, China*
Chunyan Tian − *State Key Laboratory of Medical Proteomics, Beijing Proteome Research Center, National Center for Protein Sciences (Beijing), Beijing Institute of Lifeomics, Beijing 102206, China*
Jing Yang − *Guangzhou National Laboratory, Guangzhou 510005, China; Guangzhou Municipal and Guangdong Provincial Key Laboratory of Molecular Target & Clinical Pharmacology, The NMPA and State Key Laboratory of Respiratory Disease, School of Pharmaceutical Sciences, Guangzhou Medical University, Guangzhou 511436, China*

Complete contact information is available at: https://pubs.acs.org/10.1021/jacsau.5c00244

Author Contributions

#Hui Zhang, Hailu Zhang, and C.H. contributed equally. Hui Zhang: Methodology, investigation, formal analysis. Hailu Zhang: Methodology, investigation. C.H.: Formal analysis. Q.Z.: Investigation. C.T.: Supervision. J.Y.: Supervision. F.H.: Supervision. Y.Y.: Conceptualization, supervision, writing—review & editing. CRediT: **Hui Zhang** formal analysis, investigation, methodology; **Hailu Zhang** investigation, methodology; **ChuanXi Huang** formal analysis; **Qing Zeng** investigation; **Chunyan Tian** supervision; **Jing Yang** supervision; **Fuchu He** investigation; **Yun Yang** conceptualization, supervision, writing - original draft, writing - review & editing.

Notes

The authors declare no competing financial interest.

■ ACKNOWLEDGMENTS

The authors acknowledge the assistance of Dr. Linhai Xie from National Center for Protein Sciences (Beijing) in data analysis. This work was supported by the Ministry of Science and Technology of the People's Republic of China (Grant No. 2020YFE0202200), the Prestudy Project of Phronesis Medicine Large-scale Scientific Facility funded by Guangzhou Development District, and Guangzhou National Laboratory (Grant No. GZNL2024A03001).

■ REFERENCES

(1) Rosenberger, F. A.; Thielert, M.; Mann, M. Making Single-Cell Proteomics Biologically Relevant. *Nat. Methods* **2023**, *20* (3), 320−323.
(2) Single-Cell Proteomics: Challenges and Prospects *Nat. Methods* **2023** *20* 3317 318 .
(3) Nusinow, D. P.; Szpyt, J.; Ghandi, M.; Rose, C. M.; McDonald, E. R.; Kalocsay, M.; Jané-Valbuena, J.; Gelfand, E.; Schweppe, D. K.; Jedrychowski, M.; Golji, J.; Porter, D. A.; Rejtar, T.; Wang, Y. K.; Kryukov, G. V.; Stegmeier, F.; Erickson, B. K.; Garraway, L. A.; Sellers, W. R.; Gygi, S. P. Quantitative Proteomics of the Cancer Cell Line Encyclopedia. *Cell* **2020**, *180* (2), 387−402.
(4) Zhang, H.; Ji, S.; Zhang, K.; Chen, Y.; Ming, J.; Kong, F.; Wang, L.; Wang, S.; Zou, Z.; Xiong, Z.; Xu, K.; Lin, Z.; Huang, B.; Liu, L.; Fan, Q.; Jin, S.; Deng, H.; Xie, W. Stable Maternal Proteins Underlie Distinct Transcriptome, Translatome, and Proteome Reprogramming during Mouse Oocyte-to-Embryo Transition. *Genome Biol.* **2023**, *24* (1), 166.
(5) Sun, L.; Dubiak, K. M.; Peuchen, E. H.; Zhang, Z.; Zhu, G.; Huber, P. W.; Dovichi, N. J. Single Cell Proteomics Using Frog (Xenopus Laevis) Blastomeres Isolated from Early Stage Embryos, Which Form a Geometric Progression in Protein Content. *Anal. Chem.* **2016**, *88* (13), 6653−6657.
(6) Lombard-Banek, C.; Moody, S. A.; Nemes, P. Single-Cell Mass Spectrometry for Discovery Proteomics: Quantifying Translational Cell Heterogeneity in the 16-Cell Frog (Xenopus) Embryo. *Angew. Chem., Int. Ed.* **2016**, *55* (7), 2454−2458.
(7) Li, Z. Y.; Huang, M.; Wang, X. K.; Zhu, Y.; Li, J. S.; Wong, C. C. L.; Fang, Q. Nanoliter-Scale Oil-Air-Droplet Chip-Based Single Cell Proteomic Analysis. *Anal. Chem.* **2018**, *90* (8), 5430−5438.
(8) Zhu, Y.; Clair, G.; Chrisler, W. B.; Shen, Y.; Zhao, R.; Shukla, A. K.; Moore, R. J.; Misra, R. S.; Pryhuber, G. S.; Smith, R. D.; Ansong, C.; Kelly, R. T. Proteomic Analysis of Single Mammalian Cells Enabled by Microfluidic Nanodroplet Sample Preparation and Ultrasensitive NanoLC-MS. *Angew. Chem., Int. Ed.* **2018**, *57* (38), 12370−12374.
(9) Li, Q.; Mu, L.; Yang, X.; Wang, G.; Liang, J.; Wang, S.; Zhang, H.; Li, Z. Discovery of Oogenesis Biomarkers from Mouse Oocytes Using a Single-Cell Proteomics Approach. *J. Proteome Res.* **2023**, *22* (6), 2067−2078.
(10) Huang, J.; Chen, P.; Jia, L.; Li, T.; Yang, X.; Liang, Q.; Zeng, Y.; Liu, J.; Wu, T.; Hu, W.; Kee, K.; Zeng, H.; Liang, X.; Zhou, C. Multi-Omics Analysis Reveals Translational Landscapes and Regulations in Mouse and Human Oocyte Aging. *Adv. Sci.* **2023**, *10* (26), No. 2301538.
(11) Ye, Z.; Sabatier, P.; Martin-Gonzalez, J.; Eguchi, A.; Lechner, M.; Østergaard, O.; Xie, J.; Guo, Y.; Schultz, L.; Truffer, R.; Bekker-Jensen, D. B.; Bache, N.; Olsen, J. V. One-Tip Enables Comprehensive Proteome Coverage in Minimal Cells and Single Zygotes. *Nat. Commun.* **2024**, *15* (1), No. 2474.
(12) Jiang, Y.-R.; Zhu, L.; Cao, L.-R.; Wu, Q.; Chen, J.-B.; Wang, Y.; Wu, J.; Zhang, T.-Y.; Wang, Z.-L.; Guan, Z.-Y.; Xu, Q.-Q.; Fan, Q.-X.; Shi, S.-W.; Wang, H.-F.; Pan, J.-Z.; Fu, X.-D.; Wang, Y.; Fang, Q. Simultaneous Deep Transcriptome and Proteome Profiling in a Single Mouse Oocyte. *Cell Rep.* **2023**, *42* (11), No. 113455.
(13) He, Y.; Yuan, H.; Liang, Y.; Liu, X.; Zhang, X.; Ji, Y.; Zhao, B.; Yang, K.; Zhang, J.; Zhang, S.; Zhang, Y.; Zhang, L. On-Capillary Alkylation Micro-Reactor: A Facile Strategy for Proteo-Metabolome Profiling in the Same Single Cells. *Chem. Sci.* **2023**, *14* (46), 13495−13502.
(14) Vander Borght, M.; Wyns, C. Fertility and Infertility: Definition and Epidemiology. *Clin. Biochem.* **2018**, *62*, 2−10.
(15) Sang, Q.; Ray, P. F.; Wang, L. Understanding the Genetics of Human Infertility. *Science* **2023**, *380* (6641), 158−163.
(16) Gatto, L.; Aebersold, R.; Cox, J.; Demichev, V.; Derks, J.; Emmott, E.; Franks, A. M.; Ivanov, A. R.; Kelly, R. T.; Khoury, L.; Leduc, A.; MacCoss, M. J.; Nemes, P.; Perlman, D. H.; Petelski, A. A.; Rose, C. M.; Schoof, E. M.; Van Eyk, J.; Vanderaa, C.; Yates, J. R.; Slavov, N. Initial Recommendations for Performing, Benchmarking and Reporting Single-Cell Proteomics Experiments. *Nat. Methods* **2023**, *20* (3), 375−386.
(17) Zhu, Y.; Piehowski, P. D.; Zhao, R.; Chen, J.; Shen, Y.; Moore, R. J.; Shukla, A. K.; Petyuk, V. A.; Campbell-Thompson, M.; Mathews, C. E.; Smith, R. D.; Qian, W. J.; Kelly, R. T. Nanodroplet Processing Platform for Deep and Quantitative Proteome Profiling of 10−100 Mammalian Cells. *Nat. Commun.* **2018**, *9*, No. 882.
(18) Lou, Q.; Ma, Y.; Zhao, S.-P.; Du, G.-S.; Fang, Q. A Flexible and Cost-Effective Manual Droplet Operation Platform for Miniaturized Cell Assays and Single Cell Analysis. *Talanta* **2021**, *224*, No. 121874.
(19) Woo, J.; Williams, S. M.; Markillie, L. M.; Feng, S.; Tsai, C. F.; Aguilera-Vazquez, V.; Sontag, R. L.; Moore, R. J.; Hu, D.; Mehta, H. S.; Cantlon-Bruce, J.; Liu, T.; Adkins, J. N.; Smith, R. D.; Clair, G. C.; Pasa-Tolic, L.; Zhu, Y. High-Throughput and High-Efficiency Sample Preparation for Single-Cell Proteomics Using a Nested Nanowell Chip. *Nat. Commun.* **2021**, *12* (1), No. 6246.
(20) Yang, Z.; Jin, K.; Chen, Y.; Liu, Q.; Chen, H.; Hu, S.; Wang, Y.; Pan, Z.; Feng, F.; Shi, M.; Xie, H.; Ma, H.; Zhou, H. AM-DMF-SCP: Integrated Single-Cell Proteomics Analysis on an Active Matrix Digital Microfluidic Chip. *JACS Au* **2024**, *4*, 1811−1823.
(21) Karagach, S.; Smollich, J.; Atrakchi, O.; Mohan, V.; Geiger, T.High Throughput Single-Cell Proteomics of in-Vivo Cells, 2024. https://doi.org/10.1101/2024.11.01.621461.
(22) Matzinger, M.; Müller, E.; Dürnberger, G.; Pichler, P.; Mechtler, K. Robust and Easy-to-Use One-Pot Workflow for Label-Free Single-Cell Proteomics. *Anal. Chem.* **2023**, *95* (9), 4435−4445.

(23) Isola, J. V. V.; Ocañas, S. R.; Hubbart, C. R.; Ko, S.; Mondal, S. A.; Hense, J. D.; Carter, H. N. C.; Schneider, A.; Kovats, S.; Alberola-Ila, J.; Freeman, W. M.; Stout, M. B. A Single-Cell Atlas of the Aging Mouse Ovary. *Nat. Aging* **2024**, *4* (1), 145−162.
(24) Li, M.; Ren, C.; Zhou, S.; He, Y.; Guo, Y.; Zhang, H.; Liu, L.; Cao, Q.; Wang, C.; Huang, J.; Hu, Y.; Bai, X.; Guo, X.; Shu, W.; Huo, R. Integrative Proteome Analysis Implicates Aberrant RNA Splicing in Impaired Developmental Potential of Aged Mouse Oocytes. *Aging Cell* **2021**, *20* (10), No. e13482.
(25) Dutta, S.; Sengupta, P. Men and Mice: Relating Their Ages. *Life Sci.* **2016**, *152*, 244−248.
(26) Zhang, H.; Shigang, Z.; Han, Z. Genetic Research Progress on Abnormal Development of Human Oocytes and Early Embryos. *Chin. J. Cell Biol.* **2024**, *46* (4), 646−656.
(27) Sahoo, G.; Samal, D.; Khandayataray, P.; Murthy, M. K. A Review on Caspases: Key Regulators of Biological Activities and Apoptosis. *Mol. Neurobiol.* **2023**, *60* (10), 5805−5837.
(28) De Maeyer, R. P. H.; Chambers, E. S. The Impact of Ageing on Monocytes and Macrophages. *Immunol. Lett.* **2021**, *230*, 1−10.
(29) Cao, Y.; Fan, Y.; Li, F.; Hao, Y.; Kong, Y.; Chen, C.; Hao, X.; Han, D.; Li, G.; Wang, Z.; Song, C.; Han, J.; Zeng, H. Phenotypic and Functional Alterations of Monocyte Subsets with Aging. *Immun. Ageing* **2022**, *19* (1), 63.
(30) Zeng, Q.; Gong, Y.; Zhu, N.; Shi, Y.; Zhang, C.; Qin, L. Lipids and Lipid Metabolism in Cellular Senescence: Emerging Targets for Age-Related Diseases. *Ageing Res. Rev.* **2024**, *97*, No. 102294.
(31) Smits, M. A. J.; Schomakers, B. V.; van Weeghel, M.; Wever, E. J. M.; Wüst, R. C. I.; Dijk, F.; Janssens, G. E.; Goddijn, M.; Mastenbroek, S.; Houtkooper, R. H.; Hamer, G. Human Ovarian Aging Is Characterized by Oxidative Damage and Mitochondrial Dysfunction. *Hum. Reprod.* **2023**, *38* (11), 2208−2220.
(32) Yang, Q.; Xi, Q.; Wang, M.; Long, R.; Hu, J.; Li, Z.; Ren, X.; Zhu, L.; Jin, L. Rapamycin Improves the Quality and Developmental Competence of Mice Oocytes by Promoting DNA Damage Repair during in Vitro Maturation. *Reprod. Biol. Endocrinol.* **2022**, *20* (1), 67.
(33) So, C.; Menelaou, K.; Uraji, J.; Harasimov, K.; Steyer, A. M.; Seres, K. B.; Bucevičius, J.; Lukinavičius, G.; Möbius, W.; Sibold, C.; Tandler-Schneider, A.; Eckel, H.; Moltrecht, R.; Blayney, M.; Elder, K.; Schuh, M. Mechanism of Spindle Pole Organization and Instability in Human Oocytes. *Science* **2022**, *375* (6581), No. eabj3944.
(34) Wang, S.; Zheng, Y.; Li, J.; Yu, Y.; Zhang, W.; Song, M.; Liu, Z.; Min, Z.; Hu, H.; Jing, Y.; He, X.; Sun, L.; Ma, L.; Esteban, C. R.; Chan, P.; Qiao, J.; Zhou, Q.; Izpisua Belmonte, J. C.; Qu, J.; Tang, F.; Liu, G.-H. Single-Cell Transcriptomic Atlas of Primate Ovarian Aging. *Cell* **2020**, *180* (3), 585−600.
(35) Han, Y.; Du, Z.; Wu, H.; Zhao, R.; Liu, J.; Gao, S.; Zeng, S. CALB1 and RPL23 Are Essential for Maintaining Oocyte Quality and Function During Aging. *Aging Cell* **2025**, No. e14466.
(36) Marshall, K. L.; Wang, J.; Ji, T.; Rivera, R. M. The Effects of Biological Aging on Global DNA Methylation, Histone Modification, and Epigenetic Modifiers in the Mouse Germinal Vesicle Stage Oocyte. *Anim. Reprod.* **2018**, *15* (4), 1253−1267.
(37) Zhang, G.; Zhang, N.; Zhang, B.; Zhao, Y.; Wang, Q.; Han, L. UBE2D3 Functions in Mouse Oocyte Meiotic Maturation. *FASEB J.* **2025**, *39* (3), No. e70375.
(38) Ma, J.; Chen, T.; Wu, S.; Yang, C.; Bai, M.; Shu, K.; Li, K.; Zhang, G.; Jin, Z.; He, F.; Hermjakob, H.; Zhu, Y. IProX: An Integrated Proteome Resource. *Nucleic Acids Res.* **2019**, *47* (D1), D1211−D1217.

https://doi.org/10.1021/jacsau.5c00244
JACS Au 2025, 5, 2321−2333